



This is a repository copy of *The damping of coronal loop oscillations* .

White Rose Research Online URL for this paper:  
<http://eprints.whiterose.ac.uk/1657/>

---

**Article:**

Ruderman, M.S. and Roberts, B. (2002) The damping of coronal loop oscillations. *Astrophysical Journal*, 577 (1). pp. 475-486. ISSN 1538-4365

<https://doi.org/10.1086/342130>

---

**Reuse**

Unless indicated otherwise, fulltext items are protected by copyright with all rights reserved. The copyright exception in section 29 of the Copyright, Designs and Patents Act 1988 allows the making of a single copy solely for the purpose of non-commercial research or private study within the limits of fair dealing. The publisher or other rights-holder may allow further reproduction and re-use of this version - refer to the White Rose Research Online record for this item. Where records identify the publisher as the copyright holder, users can verify any specific terms of use on the publisher's website.

**Takedown**

If you consider content in White Rose Research Online to be in breach of UK law, please notify us by emailing [eprints@whiterose.ac.uk](mailto:eprints@whiterose.ac.uk) including the URL of the record and the reason for the withdrawal request.



[eprints@whiterose.ac.uk](mailto:eprints@whiterose.ac.uk)  
<https://eprints.whiterose.ac.uk/>

## THE DAMPING OF CORONAL LOOP OSCILLATIONS

M. S. RUDERMAN

Department of Applied Mathematics, University of Sheffield, Hicks Building, Hounsfield Road, Sheffield S3 7RH, UK; m.s.ruderman@sheffield.ac.uk

AND

B. ROBERTS

School of Mathematics and Statistics, University of Saint Andrews, Saint Andrews, Fife KY16 9SS, UK

Received 2001 August 31; accepted 2002 May 22

### ABSTRACT

Motivated by recent *Transition Region and Coronal Explorer (TRACE)* observations of damped oscillations in coronal loops, we consider analytically the motion of an inhomogeneous coronal magnetic tube of radius  $a$  in a zero- $\beta$  plasma. An initially perturbed tube may vibrate in its kink mode of oscillation, but those vibrations are damped. The damping is due to resonant absorption, acting in the inhomogeneous regions of the tube, which leads to a transfer of energy from the kink mode to Alfvén (azimuthal) oscillations within the inhomogeneous layer. We determine explicitly the decrement  $\gamma$  (decay time  $\gamma^{-1}$ ) for a coronal flux tube whose plasma density varies only in a thin layer of thickness  $\ell$  on the tube boundary. The effect of viscosity is also considered. We show that, in general, the problem involves two distinct timescales,  $\gamma^{-1}$  and  $\omega_k^{-1} R^{1/3}$ , where  $R$  is the Reynolds number and  $\omega_k$  is the frequency of the kink mode. Under coronal conditions (when  $\gamma^{-1} \ll \omega_k^{-1} R^{1/3}$ ), the characteristic damping time of global oscillations is  $\gamma^{-1}$ . During this time, most of the energy in the initial perturbation is transferred into a resonant absorption layer of thickness of order  $\ell^2/a$ , with motions in this layer having an amplitude of order  $a/\ell$  times the initial amplitude. We apply our results to the observations, suggesting that loop oscillations decay principally because of inhomogeneities in the loop. Our theory suggests that only those loops with density inhomogeneities on a small scale (confined to within a thin layer of order  $a\gamma/\omega_k$  in thickness) are able to support coherent oscillations for any length of time and so be observable. Loops with a more gradual density variation, on the scale of the tube radius  $a$ , do not exhibit pronounced oscillations.

*Subject headings:* MHD — plasmas — Sun: corona — waves

### 1. INTRODUCTION

This paper has been motivated by the recent observations of standing oscillations of solar coronal loops (Aschwanden et al. 1999, 2002; Nakariakov et al. 1999; Schrijver & Brown 2000; Schrijver, Aschwanden, & Title 2002), detected by the *Transition Region and Coronal Explorer (TRACE)* spacecraft. An understanding of coronal oscillations is especially important because such oscillations may shed light on the puzzle of coronal heating, and, furthermore, they may provide seismic information about the coronal plasma (see, e.g., Roberts 2000). Aschwanden et al. (1999) and Nakariakov et al. (1999) interpreted the observed oscillations, which followed on from an earlier flare in a nearby location, in terms of the kink mode of oscillation of a coronal loop. The theory of coronal loop oscillations has been developed in some detail for the special case of a straight cylinder of magnetic field embedded in magnetized plasma surroundings (see, e.g., Edwin & Roberts 1983). Nakariakov et al. (1999) noted that the loop oscillations were strongly damped, decaying in about 14.5 minutes (compared with an oscillation period of 256 s). If such a rapid decay is due to viscous (or ohmic) damping, then the coefficient of the shear viscosity must be several orders of magnitude larger than that given by the classical Braginskii (1965) value (Nakariakov et al. 1999). On the other hand, many other effects may also bring about decay, and they require careful assessment (Roberts 2000). An understanding of what brings about the decay is an important step in understanding coronal oscilla-

tion phenomena in general, with coronal seismology a natural goal (Nakariakov & Ofman 2001).

Here we consider the manner in which energy in the global mode of oscillation of a coronal loop is transferred into motions (predominantly azimuthal) in a thin layer at the boundary of the loop where the plasma density falls from high values to match its surroundings. The process is an example of *resonant absorption*. Resonant absorption has been discussed for both *driven* systems (see, e.g., Davila 1987; Grossmann & Smith 1988; Hollweg 1990; Sakurai, Goossens, & Hollweg 1991; Goossens, Hollweg, & Sakurai 1992; Poedts & Kerner 1992; Poedts, Beliën, & Goedbloed 1994; Ofman, Davila, & Steinolfson 1994, 1995; Ofman & Davila 1995, 1996; Halberstaad & Goedbloed 1995; Poedts & Goedbloed 1997) and for *initial value problems* (e.g., Sedlacek 1971; Ionson 1978; Rae & Roberts 1982; Lee & Roberts 1986; Hollweg 1987; Hollweg & Yang 1988; Steinolfson & Davila 1993). Indeed, it may be that the observed decay of loop oscillations provides an explicit illustration of resonant absorption. By solving an initial value problem, we are able to determine the decay rate of this process. Our treatment is similar in spirit to the discussion of an incompressible transitional layer by Rae & Roberts (1982) and Lee & Roberts (1986), which in turn drew on the analysis by Sedlacek (1971) of electrostatic oscillations and by Ionson (1978) of coronal oscillations. For a weakly dissipative plasma, the decay rate that we determine is independent of dissipative coefficients; instead, the decay rate provides a direct measure of how strongly inhomogeneous is a coronal loop.

In accordance with Beaufumé, Coppi, & Golub (1992), coronal loops may be divided into three types: small, medium, and large. Typical number densities in these three types of loop are  $10^{16}$ ,  $3 \times 10^{15}$ , and  $10^{15}$ , respectively, with corresponding typical magnetic field strengths of perhaps 300, 150, and 50 G. For a coronal temperature of  $2 \times 10^6$  K, we then obtain a plasma beta  $\beta \lesssim 5 \times 10^{-4}$ . In fact, the magnitudes of magnetic fields in the corona are usually obtained by extrapolating from photospheric magnetic sources (which are themselves measured with the Zeeman effect in photospheric lines). Recently, however, Nakariakov (2001) has reported estimates of magnetic field strengths in coronal loops based on observations of loop oscillations. The lower limit for the magnetic field strength that follows from his analysis is 4 G. Thus, even if we take the number density equal to the largest value observed in coronal loops, at  $10^{16} \text{ m}^{-3}$  and a high coronal temperature of  $3 \times 10^6$  K, we obtain  $\beta \approx 0.14$ . These estimates allow us to employ the cold plasma approximation ( $\beta = 0$ ) in what follows. This approximation corresponds to the sound speed tending to zero. This is just opposite to the incompressible plasma approximation, which corresponds to the sound speed tending to infinity.

Finally, we note that *propagating* compressive waves have also been detected in coronal loops (Berghmans & Clette 1999; De Moortel, Ireland, & Walsh 2000; Robbrecht et al. 2001; O'Shea et al. 2001) and in polar plumes (Ofman et al. 1997; Ofman, Nakariakov, & DeForest 1999; DeForest & Gurman 1998). Furthermore, prominences are also observed to oscillate and indeed may exhibit *decaying* oscillations (Molowny-Hobas et al. 1999; Terradas, Oliver, & Ballester 2001) that have some similarity to the decaying coronal loop oscillations discussed here. It may be that an interpretation of the decay in prominence oscillations can be given along lines similar to those proposed here for coronal loops.

The resonant absorption considered in this paper is not the only mechanism that might explain the damping of magnetic tube oscillations. Another possible damping mechanism is radial wave leakage (e.g., Cally 1986; Stenuit, Keppens, & Goossens 1998; Stenuit et al. 1999). Such wave leakage occurs when the solution in the environment of a tube has the form of a propagating wave. However, this mechanism is not applicable to the particular case of kink oscillations of a coronal loop. This is because the leakage can only happen if the phase speed of the loop oscillation is larger than the Alfvén speed outside the loop. However, as we will see in what follows, if the plasma density in the magnetic tube is larger than the density outside the tube, as in coronal loops, then this inequality is not satisfied. Hence, kink oscillations of a coronal loop are always nonleaky.

Our paper is organized as follows. In the next section we formulate the problem and in § 3 derive the governing equation for the perturbation of the magnetic pressure, obtaining the solution to this equation in the form of a Bromwich integral. This solution is used in § 4 to study the fundamental global mode of oscillation of a magnetic tube. In § 5 the asymptotic state of the oscillation in the magnetic tube boundary is studied for times much larger than the period of the global mode. In § 6 the wave motion in the dissipative layer embracing the ideal resonant position is studied. In § 7 we compare our theoretical results with the observations of

damped oscillations of coronal loops, presenting our conclusions in § 8.

## 2. FORMULATION

We consider oscillations of a magnetic tube in a cold viscous plasma. We aim to apply our results to the oscillations of solar coronal loops. In accordance with the classical Braginskii's expression for the viscosity tensor in a magnetized plasma (Braginskii 1965), under typical coronal conditions, the coefficient of the shear viscosity is at least 10 orders of magnitude smaller than that of the compressional viscosity. However, in the problem of oscillations of coronal loops, dissipation is only important in an Alfvénic dissipative layer embracing an ideal resonant magnetic surface. Numerical studies by Ofman et al. (1994) and Erdélyi & Goossens (1995) have shown that in Alfvénic dissipative layers only the shear viscosity is significant, all other terms in Braginskii's tensorial expression being neglected. This fact enables us to write the viscous force in the momentum equation in a simplified form  $\rho\nu\nabla^2\mathbf{v}$ , where  $\mathbf{v}$  is the velocity,  $\rho$  the plasma density, and  $\nu$  the kinematic viscosity.

Inside the flux tube the plasma density is  $\rho_i$ , and outside it is  $\rho_e$ . The two regions are connected by a thin layer,  $a - \ell < r < a$  with  $\ell \ll a$ , where the plasma density varies monotonically from  $\rho_i$  to  $\rho_e$ , with  $\rho_i > \rho_e$ . The equilibrium magnetic field  $\mathbf{B}$  is everywhere uniform and in the  $z$ -direction,  $\mathbf{B} = B\hat{z}$  (see Fig. 1). The nonuniformity in plasma density  $\rho(r)$  produces a nonuniform Alfvén speed, allowing resonant wave effects to occur. It is in such nonuniform layers that viscous effects are likely to be most important.

In what follows we adopt the cylindrical coordinates  $r$ ,  $\varphi$ , and  $z$  with the  $z$ -axis aligned with the equilibrium magnetic field. In the dissipative layer, there are large gradients in the radial direction only. This observation enables us to use the approximation  $\nu\nabla^2\mathbf{v} \approx \nu\partial^2\mathbf{v}/\partial r^2$ . Then the linearized MHD

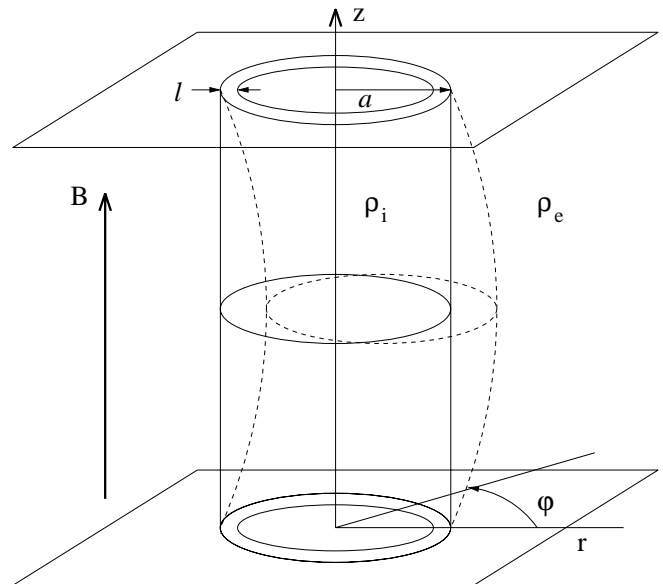


FIG. 1.—Sketch of the equilibrium state, showing a magnetic flux tube with plasma density  $\rho_i$  embedded in a plasma with density  $\rho_e$ . The equilibrium magnetic field everywhere has strength  $B$ . The equilibrium density varies in the annulus region  $a - \ell < r < a$  from  $\rho_i$  to  $\rho_e$ . The dashed lines show the perturbed magnetic tube in its kink mode of oscillation.

equations for a cold (zero  $\beta$ ) plasma take the form

$$\frac{\partial u}{\partial t} = \frac{1}{\rho} \left( \frac{B \partial b_r}{\mu \partial z} - \frac{\partial P}{\partial r} \right) + \nu \frac{\partial^2 u}{\partial r^2}, \quad (1a)$$

$$\frac{\partial v}{\partial t} = \frac{1}{\rho} \left( \frac{B \partial b_\varphi}{\mu \partial z} - \frac{1}{r} \frac{\partial P}{\partial \varphi} \right) + \nu \frac{\partial^2 v}{\partial r^2}, \quad (1b)$$

$$\frac{\partial b_r}{\partial t} = B \frac{\partial u}{\partial z}, \quad \frac{\partial b_\varphi}{\partial t} = B \frac{\partial v}{\partial z}, \quad \mathbf{\nabla} \cdot \mathbf{b} = 0, \quad (1c)$$

$$\frac{\partial P}{\partial t} = -\frac{\rho V_A^2}{r} \left[ \frac{\partial(ru)}{\partial r} + \frac{\partial v}{\partial \varphi} \right]. \quad (1d)$$

Here  $\mathbf{v} = (u, v, 0)$  is the velocity and  $\mathbf{b} = (b_r, b_\varphi, b_z)$  is the perturbed magnetic field, with  $P = Bb_z/\mu$  being the perturbation in magnetic pressure. The Alfvén speed is  $V_A(r) = B[\mu\rho(r)]^{-1/2}$ , with  $\mu$  the magnetic permeability.

We assume that the magnetic tube is bounded at  $z = 0$  and  $L$  by dense ideal infinitely conducting plasmas with the magnetic field frozen in these plasmas. This and the continuity of  $b_z$  across the boundaries imply the boundary conditions

$$u = v = 0 \quad \text{at} \quad z = 0, L. \quad (2)$$

Equation (2) coupled with equation (1d) implies that  $P = 0$  at  $z = 0, L$ .

Observations of coronal loop oscillations reported by Aschwanden et al. (1999), Nakariakov et al. (1999), and Schrijver & Brown (2000) relate to displacements of the loop axis. We consider that the disturbances causing coronal loop oscillations occur mainly at the coronal level and result in displacements of the apex part of a loop. If the amplitude of the initial displacement decreases monotonically with distance from the apex, then it is the fundamental mode of kink oscillations that is most efficiently excited. This conclusion prompts us to consider the kink oscillations of the tube, these being the only oscillations that perturb the tube axis. However, if the disturbances causing coronal loop oscillations occur mainly below the coronal level (Schrijver & Brown 2000 suggested a model where the disturbances caused by a coronal flare propagate mainly at the photospheric level and perturb the loop footpoints), then it is not clear which particular mode (with respect to the loop axis) is the most easily excited. Nevertheless, our analysis remains applicable to an overtone if we regard  $L$  as the distance between successive nodes along the loop.

In the kink mode, perturbations are proportional to  $e^{i\varphi}$  (with the coefficients of proportionality real for  $u, b_r$ , and  $P$  and purely imaginary for  $v$  and  $b_\varphi$ ). This choice corresponds to a linearly polarized kink oscillation of the tube. With our analysis restricted to the fundamental mode, it follows from the boundary conditions (2) that perturbations of  $u, v$ , and  $P$  are proportional to  $\sin(\pi z/L)$ .

Eliminating  $b_r$  and  $b_\varphi$  from equations (1a)–(1c), we obtain

$$\frac{\partial^2 u}{\partial t^2} + \omega_A^2 u - \nu \frac{\partial^3 u}{\partial t \partial r^2} = -\frac{1}{\rho} \frac{\partial^2 P}{\partial t \partial r}, \quad (3a)$$

$$\frac{\partial^2 v}{\partial t^2} + \omega_A^2 v - \nu \frac{\partial^3 v}{\partial t \partial r^2} = -\frac{i}{r\rho} \frac{\partial P}{\partial t}, \quad (3b)$$

where the Alfvén frequency is given by  $\omega_A = \pi V_A/L$ .

We need also an equation for  $P$ . Multiply equation (1a) by  $r\rho$  and differentiate the result with respect to  $r$ . Then multiply equation (1b) by  $\rho$  and differentiate the result with respect to  $\varphi$ . Adding the obtained equations, we arrive at

$$r \frac{d\rho}{dr} \frac{\partial u}{\partial t} + \rho \frac{\partial}{\partial t} \left[ \frac{\partial(ru)}{\partial r} + iv \right] = \frac{P}{r} - \frac{\partial}{\partial r} r \frac{\partial P}{\partial r} + \frac{B}{\mu} \frac{\partial}{\partial z} \left[ \frac{\partial(rb_r)}{\partial r} + ib_\varphi \right] - \nu \rho \frac{\partial^2}{\partial r^2} \left[ \frac{\partial(ru)}{\partial r} + iv \right]. \quad (4)$$

Finally, we use equation (1d) to eliminate  $v$  and the equation  $\mathbf{\nabla} \cdot \mathbf{b} = 0$  to eliminate  $b_r$  and  $b_\varphi$ . This results in

$$\frac{\partial^2 P}{\partial t^2} - \frac{V_A^2}{r} \frac{\partial}{\partial r} r \frac{\partial P}{\partial r} + \left( \omega_A^2 + \frac{V_A^2}{r^2} \right) P = V_A^2 \frac{d\rho}{dr} \frac{\partial u}{\partial t}. \quad (5)$$

Using equation (1d) to express  $v$  in terms of  $u$  and  $P$  and substituting the result into equation (3b), we obtain

$$\frac{\partial^3(ru)}{\partial t^2 \partial r} + \omega_A^2 \frac{\partial(ru)}{\partial r} - \nu \frac{\partial^4(ru)}{\partial t \partial r^3} = -\frac{r}{\rho V_A^2} \frac{\partial}{\partial t} \left[ \frac{\partial^2 P}{\partial t^2} + \left( \omega_A^2 + \frac{V_A^2}{r^2} \right) P \right]. \quad (6)$$

Note that we have neglected terms proportional to  $\nu \partial^2 P / \partial r^2$  when deriving equations (5) and (6). We can do this because viscosity is only important in the dissipative layer where there are large gradients of perturbations. However, unlike  $u$  and  $v$ ,  $P$  is almost constant across a dissipative layer (see, e.g., Goossens & Ruderman 1995), and thus no large gradients of  $P$  arise.

Equations (3a), (3b), (5), and (6) will be used in what follows to study damped oscillations of the perturbed magnetic tube. Note that these equations are not independent because there are four equations for three variables. However, it turns out that it is convenient to use equation (3a) in the regions  $r > a$  and  $r < a - \ell$ , while equation (6) is more suitable in the region  $a - \ell < r < a$ .

To complete the formulation of the problem, we have to specify initial conditions at  $t = 0$ . The basic system of equations (1a)–(1d) is a system of the first-order equations with respect to the time derivatives for the quantities  $u, v, b_r, b_\varphi$ , and  $P$ . This implies that we have to specify all these quantities at  $t = 0$ . However, in what follows, we will use only  $u, v$ , and  $P$ . It follows from equations (1a) and (1d) that we can specify  $\partial u / \partial t$  and  $\partial v / \partial t$  instead of  $b_r$  and  $b_\varphi$  at  $t = 0$ . Hence, eventually, we write the initial conditions as

$$u = u_0(r), \quad \frac{\partial u}{\partial t} = u_1(r), \quad v = v_0(r), \quad \frac{\partial v}{\partial t} = v_1(r), \quad P = P_0(r) \quad \text{at} \quad t = 0. \quad (7)$$

It follows from equations (1d) and (5) that these functions are related through

$$\frac{d}{dr} r \frac{dP_0}{dr} - \left( \frac{\pi^2 r}{L^2} + \frac{1}{r} \right) P_0 + \frac{d(r\rho u_1)}{dr} + i\rho v_1 = 0. \quad (8)$$

To solve equation (5) we also need to know  $\partial P / \partial t$  at  $t = 0$ . In accordance with equation (1d) we obtain

$$\frac{\partial P}{\partial t} = -\frac{\rho V_A^2}{r} \left[ \frac{\partial(ru_0)}{\partial r} + iv_0 \right] \equiv P_1(r) \quad \text{at} \quad t = 0. \quad (9)$$

We assume that all perturbations vanish as  $r \rightarrow \infty$  and impose the condition  $u_0, u_1, v_0, v_1, P_0 \rightarrow 0$  as  $r \rightarrow \infty$ . Note that  $u_0, u_1, P_0$ , and  $P_1$  are real while  $v_0$  and  $v_1$  are purely imaginary.

It turns out in what follows that the asymptotic state of a loop oscillation is determined by the complex frequency of the eigenmode of the viscous MHD equations. However, we cannot draw this conclusion a priori. The main point of concern is that the time necessary for motions in the vicinity of the ideal resonant position to reach a steady state is much larger than the characteristic time required for the global motion of the loop to be described by its eigenmode. Hence, to conclude that global loop motions for times much larger than the eigenmode period are described by the eigenmode, it is necessary first to solve the initial value problem and then carry out an asymptotic analysis of the solution.

### 3. SOLUTION FOR THE PERTURBATION OF THE MAGNETIC PRESSURE

To obtain the solution for the perturbation of the magnetic pressure, we first derive the governing equation for it. We do this in steps. First we obtain its solution in the external region ( $r > a$ ) and in the internal region ( $r < a - \ell$ ), and then in the annulus ( $a - \ell < r < a$ ). Finally, we match these solutions at the boundaries.

#### 3.1. The External Region

The perturbation of the total pressure in the region  $r > a$  where  $\rho$  is uniform is described by equation (5) with zero right-hand side. The only quantity that we need in what follows is  $\partial P / \partial r$  at  $r = a$ . Introduce the Laplace transform

$$\mathcal{L}[f(t)](\omega) = \int_0^\infty f(t)e^{i\omega t} dt. \tag{10}$$

Applying this transform to equation (5) with  $d\rho/dr = 0$  and making the variable substitution

$$Q_e = \mathcal{L}[P] - \mathcal{L}[A_e] \frac{K_1(\pi r/L)}{K_1(\pi a/L)}, \tag{11}$$

where  $A_e(t) = P(t, a)$  and  $K_1$  is the modified Bessel (Macdonald) function of the first order, we obtain

$$\begin{aligned} \frac{1}{r} \frac{\partial}{\partial r} r \frac{\partial Q_e}{\partial r} - \left[ \frac{1}{r^2} + \frac{\pi^2}{L^2} \left( 1 - \frac{\omega^2}{\omega_{Ae}^2} \right) \right] Q_e \\ = - \frac{P_1 - i\omega P_0}{V_{Ae}^2} - \frac{\omega^2 K_1(\pi r/L)}{V_{Ae}^2 K_1(\pi a/L)} \mathcal{L}[A_e]. \end{aligned} \tag{12}$$

The quantity  $Q_e(r; \omega)$  satisfies the boundary conditions

$$Q_e(a; \omega) = 0, \quad Q_e(r; \omega) \rightarrow 0 \quad \text{as } r \rightarrow \infty. \tag{13}$$

The two linearly independent solutions to the homogeneous counterpart of equation (12) are  $I_1(r\zeta_e)$  and  $K_1(r\zeta_e)$ , where  $I_1$  is the modified Bessel function of the first order and  $\zeta_e = V_{Ae}^{-1}(\omega_{Ae}^2 - \omega^2)^{1/2}$ . The function  $\zeta_e(\omega)$  has two branch points,  $\omega = \pm\omega_{Ae}$ , and so do the functions  $I_1(r\zeta_e)$  and  $K_1(r\zeta_e)$ . To obtain single-valued branches of these functions, we make cuts in the complex  $\omega$ -plane that start from  $-\omega_{Ae}$  and  $\omega_{Ae}$  and go along the

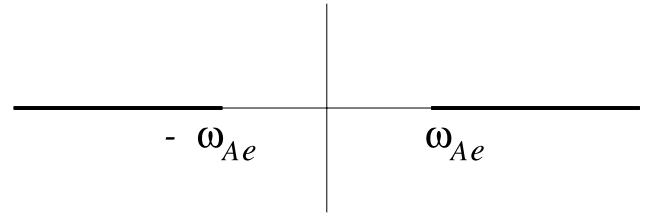


FIG. 2.—Complex  $\omega$ -plane with two cuts shown by the bold lines. The function  $\zeta_e(\omega)$  is single-valued in this plane. Similar cuts in the complex  $\omega$ -plane, although from  $-\omega_{Ae}$  and  $\omega_{Ae}$ , are used to make the functions  $\zeta_i(\omega)$  single-valued.

real axis to  $-\infty$  and  $\infty$ , respectively (see Fig. 2). One of the branches of the function  $\zeta_e(\omega)$  maps the complex plane with the two cuts on the right half of the complex plane, and the other on the left half. We choose the first branch, so that  $\Re(\zeta_e(\omega)) > 0$ , where  $\Re$  indicates the real part of a quantity. The function  $K_1(z)$  has a logarithmic branch point at  $z = 0$ . We choose a branch of  $K_1(z)$  that takes real values when  $z > 0$ . Then it follows from the asymptotic formulae (Abramowitz & Stegun 1964)

$$I_1(z) \sim \frac{e^z}{(2\pi z)^{1/2}}, \quad K_1(z) \sim \left(\frac{\pi}{2z}\right)^{1/2} e^{-z}, \tag{14}$$

valid for  $|\arg z| < \pi/2$  and  $|z| \rightarrow \infty$ , that  $I_1(r\zeta_e) \rightarrow \infty$  and  $K_1(r\zeta_e) \rightarrow 0$  as  $r \rightarrow \infty$  for any value of  $\omega$  that is not on one of the two cuts.

The Green's function of equation (12),  $G_e(r, s; \omega)$ , has to satisfy the homogeneous counterpart of equation (12) for  $r \neq s$ , the boundary conditions (13), and be continuous at  $r = s$  with jump condition

$$\lim_{\epsilon \rightarrow +0} \left( \frac{\partial G_e}{\partial r} \Big|_{r=s+\epsilon} - \frac{\partial G_e}{\partial r} \Big|_{r=s-\epsilon} \right) = 1. \tag{15}$$

Using the identity (Abramowitz & Stegun 1964)

$$I_1'(z)K_1(z) - I_1(z)K_1'(z) = \frac{1}{z}, \tag{16}$$

where the prime indicates a derivative, it is straightforward to show that  $G_e(r, s; \omega)$  is given by

$$\begin{aligned} G_e(r, s; \omega) = \frac{s}{K_1(a\zeta_e)} \left\{ H(s-r)K_1(s\zeta_e) \right. \\ \times \left[ K_1(r\zeta_e)I_1(a\zeta_e) - I_1(r\zeta_e)K_1(a\zeta_e) \right] \\ + H(r-s)K_1(r\zeta_e) \\ \left. \times \left[ K_1(s\zeta_e)I_1(a\zeta_e) - I_1(s\zeta_e)K_1(a\zeta_e) \right] \right\}, \end{aligned} \tag{17}$$

where  $H(x)$  is the Heaviside function,  $H(x) = 1$  for  $x > 0$ , and  $H(x) = 0$  for  $x < 0$ . Then the solution to equation (12), satisfying the boundary conditions (13), is

$$\begin{aligned} Q_e(r; \omega) = - \int_a^\infty G_e(r, s; \omega) \\ \times \left\{ \frac{P_1(s) - i\omega P_0(s)}{V_{Ae}^2} + \frac{\omega^2 K_1(\pi s/L)}{V_{Ae}^2 K_1(\pi a/L)} \mathcal{L}[A_e] \right\} ds. \end{aligned} \tag{18}$$

It follows from equations (11), (16), (17), and (18) that

$$\begin{aligned} \left. \frac{\partial \mathcal{L}[P]}{\partial r} \right|_{r=a} &= \int_a^\infty \frac{sK_1(s\zeta_e)}{aK_1(a\zeta_e)} \\ &\times \left\{ \frac{P_1(s) - i\omega P_0(s)}{V_{Ae}^2} + \frac{\omega^2 K_1(\pi s/L)}{V_{Ae}^2 K_1(\pi a/L)} \mathcal{L}[A_e] \right\} ds \\ &+ \frac{\pi K_1'(\pi a/L)}{LK_1(\pi a/L)} \mathcal{L}[A_e]. \end{aligned} \quad (19)$$

Using the modified Bessel equation, it is straightforward to derive the relation

$$\begin{aligned} \int_a^\infty K_1(\pi s/L) K_1(s\zeta_e) s ds &= \frac{aV_{Ae}^2}{\omega^2} \\ &\times \left[ \zeta_e K_1(\pi a/L) K_1'(a\zeta_e) - \frac{\pi}{L} K_1(a\zeta_e) K_1'(\pi a/L) \right], \end{aligned} \quad (20)$$

which allows us to rewrite equation (19) as

$$\begin{aligned} \left. \frac{\partial \mathcal{L}[P]}{\partial r} \right|_{r=a} &= \frac{1}{V_{Ae}^2} \int_a^\infty \frac{sK_1(s\zeta_e)}{aK_1(a\zeta_e)} [P_1(s) - i\omega P_0(s)] ds \\ &+ \frac{\zeta_e K_1'(a\zeta_e)}{K_1(a\zeta_e)} \mathcal{L}[A_e]. \end{aligned} \quad (21)$$

Applying the Laplace transform to equation (3a) and neglecting viscosity in the external region, we obtain

$$\begin{aligned} \mathcal{L}[u_e] &= \frac{1}{\omega_{Ae}^2 - \omega^2} \\ &\times \left\{ \frac{1}{\rho_e} \left. \frac{dP_0}{dr} \right|_{r=a} + \frac{i\omega}{\rho_e} \left. \frac{\partial \mathcal{L}[P]}{\partial r} \right|_{r=a} + u_1(a) - i\omega u_0(a) \right\}, \end{aligned} \quad (22)$$

where  $u_e = u(t, a)$ .

### 3.2. The Internal Region

The perturbation of the total pressure in the region  $r < a - \ell = b$  is described by equation (5) with zero right-hand side. We need only calculate  $\partial \mathcal{L}[P]/\partial r$  at  $r = b$  from this equation. Applying the Laplace transform to equation (5) and making the variable substitution

$$Q_i = \mathcal{L}[P] - \mathcal{L}[A_i] \frac{I_1(\pi r/L)}{I_1(\pi b/L)}, \quad (23)$$

where  $A_i(t) = P(t, b)$ , we obtain

$$\begin{aligned} \frac{1}{r} \frac{\partial}{\partial r} r \frac{\partial Q_i}{\partial r} - \left[ \frac{1}{r^2} + \frac{\pi^2}{L^2} \left( 1 - \frac{\omega^2}{\omega_{Ai}^2} \right) \right] Q_i \\ = - \frac{P_1 - i\omega P_0}{V_{Ai}^2} - \frac{\omega^2 I_1(\pi r/L)}{V_{Ai}^2 I_1(\pi b/L)} \mathcal{L}[A_i]. \end{aligned} \quad (24)$$

The quantity  $Q_i(r; \omega)$  satisfies the boundary condition

$$Q_i(b; \omega) = 0, \quad (25)$$

and, in addition, it must be regular at  $r = 0$ . Taking into account that  $I_1(z)$  is regular at  $r = 0$  and  $K_1(z)$  is singular, we find that the Green's function of equation (24) is

$$\begin{aligned} G_i(r, s; \omega) &= \frac{s}{I_1(b\zeta_i)} \left\{ H(s-r) I_1(r\zeta_i) \right. \\ &\times \left[ I_1(s\zeta_i) K_1(b\zeta_i) - K_1(s\zeta_i) I_1(b\zeta_i) \right] \\ &+ H(r-s) I_1(s\zeta_i) \\ &\left. \times \left[ I_1(r\zeta_i) K_1(b\zeta_i) - K_1(r\zeta_i) I_1(b\zeta_i) \right] \right\}, \end{aligned} \quad (26)$$

where  $\zeta_i = V_{Ai}^{-1}(\omega_{Ai}^2 - \omega^2)^{1/2}$ . Similar to the function  $\zeta_e(\omega)$ , the function  $\zeta_i(\omega)$  has two branch points,  $\omega = \pm \omega_{Ai}$ , and so do the functions  $I_1(r\zeta_i)$  and  $K_1(r\zeta_i)$ . To obtain single-valued branches of these functions, we make cuts in the complex  $\omega$ -plane that start from  $-\omega_{Ai}$  and  $\omega_{Ai}$  and go along the real axis to  $-\infty$  and  $\infty$ , respectively (see Fig. 2). One of the branches of the function  $\zeta_i(\omega)$  maps the complex plane with the two cuts on the right half of the complex plane, and the other on the left half. We choose the first branch, so that  $\Re(\zeta_i(\omega)) > 0$ . Once again we choose a branch of  $K_1(z)$  that takes real values when  $z > 0$ .

The solution to equation (24), satisfying the boundary conditions (25) and regular at  $r = 0$ , is

$$\begin{aligned} Q_i(r; \omega) &= - \int_0^b G_i(r, s; \omega) \\ &\times \left\{ \frac{P_1(s) - i\omega P_0(s)}{V_{Ai}^2} + \frac{\omega^2 I_1(\pi s/L)}{V_{Ai}^2 I_1(\pi b/L)} \mathcal{L}[A_i] \right\} ds. \end{aligned} \quad (27)$$

It follows from equations (16), (23), (26), and (27) that

$$\begin{aligned} \left. \frac{\partial \mathcal{L}[P]}{\partial r} \right|_{r=b} &= - \int_0^b \frac{s I_1(s\zeta_i)}{b I_1(b\zeta_i)} \\ &\times \left\{ \frac{P_1(s) - i\omega P_0(s)}{V_{Ai}^2} + \frac{\omega^2 I_1(\pi s/L)}{V_{Ai}^2 I_1(\pi b/L)} \mathcal{L}[A_i] \right\} ds \\ &+ \frac{\pi I_1'(\pi b/L)}{L I_1(\pi b/L)} \mathcal{L}[A_i]. \end{aligned} \quad (28)$$

Using the modified Bessel equation, it is straightforward to derive the relation

$$\begin{aligned} \int_0^b I_1(\pi s/L) I_1(s\zeta_i) s ds \\ = \frac{bV_{Ai}^2}{\omega^2} \left[ \frac{\pi}{L} I_1(b\zeta_i) I_1'(\pi b/L) - \zeta_i I_1(\pi b/L) I_1'(b\zeta_i) \right]. \end{aligned} \quad (29)$$

Using this relation, we rewrite equation (28) as

$$\begin{aligned} \left. \frac{\partial \mathcal{L}[P]}{\partial r} \right|_{r=b} &= - \frac{1}{V_{Ai}^2} \int_0^b \frac{s I_1(s\zeta_i)}{b I_1(b\zeta_i)} [P_1(s) - i\omega P_0(s)] ds \\ &+ \frac{\zeta_i I_1'(b\zeta_i)}{I_1(b\zeta_i)} \mathcal{L}[A_i]. \end{aligned} \quad (30)$$

Applying the Laplace transform to equation (3a) and neglecting viscosity in the internal region, we obtain

$$\mathcal{L}[u_i] = \frac{1}{\omega_{Ai}^2 - \omega^2} \times \left\{ \frac{1}{\rho_i} \frac{dP_0}{dr} \Big|_{r=b} + \frac{i\omega}{\rho_i} \frac{\partial \mathcal{L}[P]}{\partial r} \Big|_{r=b} + u_1(b) - i\omega u_0(b) \right\}, \quad (31)$$

where  $u_i = u(t, b)$ .

### 3.3. The Solution in the Annulus

In what follows we assume that the characteristic scale of variation of perturbations of all quantities is initially  $a$ . This implies that we can take  $u_0(b) \approx u_0(a)$ ,  $u_1(b) \approx u_1(a)$ , and so on. It follows from equation (3a) that  $u \sim P(\rho\ell\omega_A)^{-1}$ . Then it is straightforward to get from equation (5) that  $\partial^2 P/\partial r^2 \sim P(al)^{-1}$ , which implies that  $P(t, r) = A(t) + \mathcal{O}(\ell/a)$ . Hence, we can neglect variations of  $P$  in the annulus. In particular,  $A_e(t) \approx A_i(t) \approx A(t)$ . This approximation significantly simplifies the analysis. It was first used by Hollweg (1987) and subsequently by Hollweg & Yang (1988) to study resonant absorption of MHD surface waves in a thin inhomogeneous layer. Recently, it was used by Ruderman & Wright (2000) to study nonstationary driven oscillations of a thin planar magnetic cavity.

Since  $P$  is determined by its values at the annulus boundaries, we can consider equation (6) as an equation with known right-hand side. It determines  $\partial(ru)/\partial r$  for  $b < r < a$ . If we introduce the notation  $V_1 = \partial(ru)/\partial r$  and denote the right-hand side of equation (6) as  $(2/\pi)g(t, r)$ , then we obtain an equation that exactly coincides with equation (13) by Ruderman (1999) with  $n = 1$  and  $\eta = 0$ . This enables us to immediately write down an approximate solution to equation (6):

$$\frac{\partial(ru)}{\partial r} = \exp(-\Lambda t^3/R) \left[ \frac{d(ru_0)}{dr} \cos(\omega_A t) + \frac{d(ru_1)}{dr} \frac{\sin(\omega_A t)}{\omega_A} \right] - \frac{a}{\rho V_A^2} \int_0^t G(t - \tau) \frac{d}{d\tau} \left[ \frac{d^2 A}{d\tau^2} + \left( \omega_A^2 + \frac{V_A^2}{a^2} \right) A \right] d\tau. \quad (32)$$

Here  $\Lambda = \frac{1}{6} a V_{Ae} (d\omega_A/dr)^2$ ,  $R = a V_{Ae}/\nu$  is the viscous Reynolds number based upon the Alfvén speed  $V_{Ae}$ , and the Green's function  $G(t)$  is given by

$$G(t) = H(t) \exp(-\Lambda t^3/R) \frac{\sin(\omega_A t)}{\omega_A}. \quad (33)$$

Note that, since all equilibrium quantities are assumed to be smooth functions,  $\Lambda(a) = \Lambda(b) = 0$ . When writing down equation (32), we have taken  $r \approx a$  in the last term on the right-hand side. The corresponding solution was obtained by Ruderman (1999) using the WKB method with  $R^{-1/3}$  as a small parameter. Hence, the approximate solution (32) is valid for only large values of the Reynolds number  $R$ .

Let us calculate the Laplace transform of  $\partial(ru)/\partial r$ . To do this we introduce the incomplete  $F$ -function as

$$\tilde{F}(x, t) = \int_0^t \exp(ixs - s^3/3) ds \quad (34)$$

and the complete  $F$ -function as  $F(x) = \tilde{F}(x, \infty)$ . The latter

function was first introduced by Boris (1968, p. 172); it has been used to describe wave motion in dissipative layers (Mok & Einaudi 1985; Goossens, Ruderman, & Hollweg 1995; Goossens & Ruderman 1995). It is straightforward to obtain the relation

$$\mathcal{L}[\exp(\pm i\omega_A t - \Lambda t^3/R)](\omega) = \delta_\omega^{-1} F((\omega \pm \omega_A)/\delta_\omega), \quad (35)$$

where  $\delta_\omega = (3\Lambda/R)^{1/3}$ . It follows from equation (1d) that

$$\frac{\partial^2 P}{\partial t^2} \Big|_{t=0} = -\frac{\rho V_A^2}{r} \left[ \frac{\partial(ru_1)}{\partial r} + iv_1 \right] \equiv P_2(r). \quad (36)$$

Using equations (35) and (36) and the convolution theorem, we eventually arrive at

$$\begin{aligned} \frac{\partial(r\mathcal{L}[u])}{\partial r} = & \frac{1}{2\delta_\omega} \left\{ \left[ \frac{d(ru_0)}{dr} - \frac{i}{\omega_A} \frac{d(ru_1)}{dr} \right] F((\omega + \omega_A)/\delta_\omega) \right. \\ & + \left. \left[ \frac{d(ru_0)}{dr} + \frac{i}{\omega_A} \frac{d(ru_1)}{dr} \right] F((\omega - \omega_A)/\delta_\omega) \right\} \\ & + ia \frac{F((\omega + \omega_A)/\delta_\omega) - F((\omega - \omega_A)/\delta_\omega)}{2\rho V_A^2 \omega_A \delta_\omega} \\ & \times \left\{ \left( \omega^2 - \omega_A^2 - \frac{V_A^2}{a^2} \right) (i\omega \mathcal{L}[A] + A_0) \right. \\ & \left. - A_2 + i\omega A_1 \right\}, \quad (37) \end{aligned}$$

where  $A_0$ ,  $A_1$ , and  $A_2$  are the values of  $A$ ,  $dA/dt$ , and  $d^2A/dt^2$ , respectively, at  $t = 0$ ; in turn, these are approximately equal to  $P_0$ ,  $P_1$ , and  $P_2$  at  $r = a$ .

### 3.4. Matching Solutions

Integrating equation (37) with respect to  $r$  from  $b$  to  $a$ , we obtain the Laplace transform of the quantity  $au_e - bu_i$ . On the other hand, we can calculate this quantity using equations (22) and (31). Comparing the two expressions, taking into account equations (21) and (30), and substituting  $A$  for  $A_e$  and  $A_i$ , we arrive at the following expression for  $\mathcal{L}[A]$ :

$$\mathcal{L}[A] = \frac{W(\omega; R)}{D(\omega; R)}, \quad (38)$$

where

$$\begin{aligned} D(\omega; R) &= D_0(\omega) + D_1(\omega; R), \\ W(\omega; R) &= W_0(\omega) + W_1(\omega; R), \quad (39) \end{aligned}$$

$$D_0(\omega) = \frac{b\zeta_i I_1'(b\zeta_i)}{\rho_i(\omega^2 - \omega_{Ai}^2) I_1(b\zeta_i)} - \frac{a\zeta_e K_1'(a\zeta_e)}{\rho_e(\omega^2 - \omega_{Ae}^2) K_1(a\zeta_e)}, \quad (40)$$

$$\begin{aligned} D_1(\omega; R) &= \frac{ia}{2\rho V_A^2} \int_b^a \left( \omega_A^2 - \omega^2 + \frac{V_A^2}{a^2} \right) \\ &\times \frac{F((\omega + \omega_A)/\delta_\omega) - F((\omega - \omega_A)/\delta_\omega)}{\omega_A \delta_\omega} dr, \quad (41) \end{aligned}$$

$$\begin{aligned}
W_0(\omega) = & \int_0^b \frac{sI_1(s\zeta_i) P_1(s) - i\omega P_0(s)}{I_1(b\zeta_i) \rho V_A^2(\omega^2 - \omega_{Ai}^2)} ds \\
& + \int_a^\infty \frac{sK_1(s\zeta_e) P_1(s) - i\omega P_0(s)}{K_1(a\zeta_e) \rho V_A^2(\omega^2 - \omega_{Ae}^2)} ds \\
& + \frac{ib}{\omega(\omega^2 - \omega_{Ai}^2)} \left[ \frac{1}{\rho_i} \frac{dP_0}{dr} \Big|_{r=b} + u_1(b) - i\omega u_0(b) \right] \\
& - \frac{ia}{\omega(\omega^2 - \omega_{Ae}^2)} \left[ \frac{1}{\rho_e} \frac{dP_0}{dr} \Big|_{r=a} + u_1(a) - i\omega u_0(a) \right].
\end{aligned} \tag{42}$$

It can be shown that  $W_1(\omega; R)/W_0(\omega) \sim \ell/a \ll 1$ . Therefore,  $W_1(\omega; R)$  can be neglected in comparison with  $W_0(\omega)$ , and we do not give the expression for this quantity.

The functions  $D_0(\omega)$  and  $W_0(\omega)$  are multivalued and have four branch points:  $\omega = \pm\omega_{Ae}$  and  $\omega = \pm\omega_{Ai}$ . To obtain their single-valued branches we make the cuts in the complex  $\omega$ -plane from  $-\omega_{Ai}$  to  $-\infty$  and from  $\omega_{Ai}$  to  $\infty$  as shown in Figure 2 and consider the branches of  $\zeta_e(\omega)$ ,  $\zeta_i(\omega)$ , and  $K_1(z)$  determined in §§ 3.1 and 3.2. Since  $\omega_{Ai} < \omega_{Ae}$ , both  $\zeta_e(\omega)$  and  $\zeta_i(\omega)$  are single valued in the  $\omega$ -plane with these cuts.

#### 4. WEAKLY DAMPED EIGENMODES

The complex frequencies of the loop oscillations are determined by the equation

$$D(\omega; R) = 0. \tag{43}$$

If  $\omega$  is a solution to equation (43), then the dependence of the corresponding eigenfunction on  $r$  in the region  $r > a$  is given by equations (11), (17), and (18) with  $P_0 = P_1 = 0$  and  $\mathcal{L}[A_e]$  arbitrary. The quantity  $\omega$  is a true eigenfrequency because the corresponding eigenfunction tends to zero exponentially as  $r \rightarrow \infty$ , and, consequently, it is square integrable.

It is straightforward to obtain the estimate  $D_1(\omega; R)/D_0(\omega) = \mathcal{O}(\ell/a)$ . This estimate enables us to use the regular perturbation method and look for a solution to equation (43) in the form  $\omega = \omega_0 + \omega_1$ , where  $|\omega_1| \ll |\omega_0|$ . In the first-order approximation we obtain

$$D_0(\omega_0) = 0. \tag{44}$$

Now coronal loops are much thinner than they are long, so that  $a \ll L$ . Then  $|a\zeta_e| \ll 1$  and  $|b\zeta_i| \ll 1$ , and we can use the approximate formulae (Abramowitz & Stegun 1964)

$$I_1(z) \approx \frac{z}{2}, \quad I_1'(z) \approx \frac{1}{2}, \quad K_1(z) \approx \frac{1}{z}, \quad K_1'(z) \approx -\frac{1}{z^2} \tag{45}$$

to rewrite the expression (40) as

$$D_0(\omega) = \frac{1}{\rho_i(\omega^2 - \omega_{Ai}^2)} + \frac{1}{\rho_e(\omega^2 - \omega_{Ae}^2)}. \tag{46}$$

Then the solution to equation (44) is

$$\omega = \omega_0 = \pm\omega_k \equiv \pm \left( \frac{2\rho\omega_A^2}{\rho_e + \rho_i} \right)^{1/2}. \tag{47}$$

The quantity  $\omega_k$  is the frequency of kink oscillations of a thin homogeneous magnetic tube and has been discussed in

Edwin & Roberts (1983) and Roberts (2000). It was used by Nakariakov (2000) and Nakariakov & Ofman (2001) to calculate the magnetic field strength in the coronal loops by comparing the observed oscillations with theory.

In the second-order approximation we obtain

$$\omega_1 = -D_1(\omega_0; R) \left( \frac{\partial D_0}{\partial \omega} \Big|_{\omega=\omega_0} \right)^{-1}. \tag{48}$$

Using integration by parts, we obtain

$$F((\omega_0 \pm \omega_A)/\delta_\omega) \approx \frac{i\delta_\omega}{\omega_0 \pm \omega_A}, \tag{49}$$

valid when  $|\omega_0 \pm \omega_A| \gg \delta_\omega$ . However, since  $\omega_{Ae}^2 < \omega_0^2 < \omega_{Ai}^2$ , there is a location  $r = r_A$ , called the Alfvén resonant position, at which  $\omega_A^2(r_A) = \omega_0^2$ . For  $\omega_A^2(r)$  monotonic, this position is unique. Let us introduce the thickness of the Alfvén dissipative layer  $\delta_A$  as (e.g., Goossens & Ruderman 1995; Goossens et al. 1995)

$$\delta_A = \frac{2|\omega_0|\delta_\omega(r_A)}{|\Delta|} = \left| \frac{\nu\omega_0}{\Delta} \right|^{1/3}, \quad \Delta = - \frac{d\omega_A^2}{dr} \Big|_{r=r_A}. \tag{50}$$

Now we take  $s_A$  such that  $\delta_A \ll s_A \ll \ell$  and write the integral in equation (41) as a sum of integrals over  $[b, r_A - s_A]$ ,  $[r_A - s_A, r_A + s_A]$ , and  $[r_A + s_A, a]$ . Then we use the approximate expression (49) to calculate the first and third integrals. To calculate the second integral we use the approximate formula

$$|\omega_0| - \omega_A \approx \frac{\Delta(r - r_A)}{2|\omega_0|} \tag{51}$$

and neglect the nonresonant term, which is proportional to  $F(\pm(\omega_k + \omega_A)/\delta_\omega)$ . Since  $\omega_A^2 \sim \omega_0^2 \ll V_A^2 a^{-2}$ , we can take  $\omega_A^2 - \omega_0^2 + V_A^2 a^{-2} \approx V_A^2 a^{-2}$  in the integrand in equation (41). Making the substitution  $s = \delta_A^{-1}(r - r_A)\text{sgn}(\Delta\omega_0)$  in the second integral, we eventually arrive at the following approximate expression:

$$\begin{aligned}
D_1(\omega_0; R) \approx & \frac{1}{a} \left( \int_b^{r_A - s_A} + \int_{r_A + s_A}^a \right) \frac{dr}{\rho(\omega_0^2 - \omega_A^2)} \\
& - \frac{i\omega_0}{\rho_A a |\omega_0 \Delta|} \int_{-s_A/\delta_A}^{s_A/\delta_A} F(s) ds,
\end{aligned} \tag{52}$$

where  $\rho_A = \rho(r = r_A)$ . Since  $s_A \ll a - b = \ell$  and  $s_A \gg \delta_A$ , we take  $s_A \rightarrow +0$  and  $s_A/\delta_A \rightarrow \infty$ . Then, using the formula  $\int_{-\infty}^{\infty} F(s) ds = \pi$ , we obtain

$$D_1(\omega_0; R) \approx \frac{1}{a} \mathcal{P} \int_b^a \frac{dr}{\rho(\omega_0^2 - \omega_A^2)} - \frac{i\pi\omega_0}{\rho_A a |\omega_0 \Delta|}, \tag{53}$$

where  $\mathcal{P}$  indicates the principal Cauchy part of an integral. With the use of equations (46), (48), and (53), we finally obtain

$$\omega_1 = \omega_{1r} - i\gamma, \tag{54}$$

where

$$\omega_{1r} = \frac{\rho_A^2 \omega_0^3 (\rho_i - \rho_e)^2}{2a(\rho_i + \rho_e)^3} \mathcal{P} \int_b^a \frac{dr}{\rho(\omega_0^2 - \omega_A^2)}, \tag{55}$$

$$\gamma = \frac{\pi \rho_A |\omega_0|^3 (\rho_i - \rho_e)^2}{2a |\Delta| (\rho_i + \rho_e)^3}. \tag{56}$$

Note that the decrement  $\gamma$  is always positive, as it should be. It is straightforward to show that  $\omega_{1r}/\omega_0 = \mathcal{O}(\ell/a) \ll 1$ , so that we can neglect  $\omega_{1r}$  in comparison with  $\omega_0$  in the expression for  $\omega_0 + \omega_1$ . The same estimate is valid for  $\gamma/\omega_0$ , though we cannot neglect  $-i\gamma$  in the expression for  $\omega_0 + \omega_1$  because it describes damping of oscillations due to resonant absorption in the dissipative layer embracing  $r_A$ .

It is interesting to note (M. Goossens 2002, private communication) that expression (56) can be obtained as a particular case from a more general expression for the damping rate given by Goossens et al. (1992; see their eq. [77]), correcting for a typographical error in their equation). Expression (56) is also similar to expressions for the damping rate of surface waves on a finite-thickness single interface (see, e.g., Ionson 1978; Mok & Einaudi 1985; Lee & Roberts 1986; Hollweg 1987; Hollweg & Yang 1988), although it differs from these studies in that our result involves the radius of the flux tube as well as the scale of the inhomogeneity. The fact that the damping rate  $\gamma$  is independent of  $R$  (assumed large) is not surprising—it is found in previous analytical studies of such wave problems—although it is an important property of resonant absorption. This property is also confirmed by numerical studies (e.g., Poedts & Kerner 1991; Tirry & Goossens 1996). The damping timescale  $\gamma^{-1}$  is generally much shorter than the timescale by which small-scale disturbances in the resonance layer dissipate; in phase mixing and in steadily driven resonant absorption, small-scale disturbances damp on a timescale proportional to  $R^{1/3}$  (e.g., Heyvaerts & Priest 1983; Kappraff & Tataronis 1977), which is very long under coronal conditions. Consequently, it is the shorter timescale,  $\gamma^{-1}$ , that will be most apparent in observations.

### 5. OSCILLATIONS OF THE MAGNETIC TUBE BOUNDARY

In this section we study the asymptotic state of the motion of the magnetic tube boundary for  $t \gg \omega_k^{-1}$ . We start from studying the asymptotic state of the total pressure oscillation in the annulus  $b < r < a$  and then consider the annulus displacement.

#### 5.1. The Asymptotic State of the Total Pressure Oscillation

Since  $\mathcal{L}[A](\omega)$  is an analytic function in the half-plane  $\Im(\omega) > 0$  ( $\Im$  indicates the imaginary part of a quantity), it follows from equation (38) that

$$A(t) = \frac{1}{2\pi} \int_{-\infty+i\varsigma}^{\infty+i\varsigma} \frac{W_0(\omega)}{D(\omega; R)} e^{-i\omega t} d\omega, \tag{57}$$

where  $\varsigma$  is an arbitrary positive constant and we have taken into account that  $|W_1| \ll |W_0|$ . To evaluate the integral in equation (57), we close the Bromwich integration contour as shown in Figure 3. When the radius of the semicircle is large enough, the integral over the closed contour is equal to the sum of the residues of the integrand with respect to poles in the lower half-plane multiplied by  $-2\pi i$ .

Both  $W_0(\omega)$  and  $D(\omega; R)$  have simple poles at  $\omega = \pm\omega_{Ae}$  and  $\omega = \pm\omega_{Ai}$ , so their ratio is regular at these points. The function  $D(\omega; R)$  has simple poles at  $\omega = \omega_d$  and  $\omega = -\omega_d^*$ .

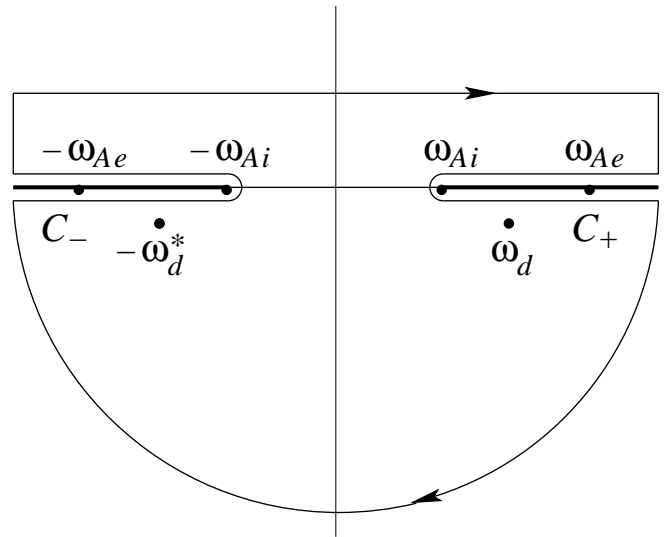


FIG. 3.—Sketch of the integration contour used to evaluate the integral in eq. (57). The arrows on the contour show the direction of integration.

Hence, the integral over the closed contour is equal to the sum of residues with respect to  $\omega = \omega_d$  and  $\omega = -\omega_d^*$  multiplied by  $-2\pi i$ .

It is straightforward to show that the integral over the semicircle tends to zero when its radius tends to infinity. As a result we obtain the expression for  $A(t)$  valid for  $t \gg \omega_k^{-1}$ :

$$A(t) = -i \left\{ \text{res}_{\omega=\omega_d} \left( \frac{W_0(\omega)}{D(\omega; R)} e^{-i\omega t} \right) + \text{res}_{\omega=-\omega_d^*} \left( \frac{W_0(\omega)}{D(\omega; R)} e^{-i\omega t} \right) \right\} - \frac{1}{2\pi} \left( \int_{\mathcal{C}_-} + \int_{\mathcal{C}_+} \right) \frac{W_0(\omega)}{D(\omega; R)} e^{-i\omega t} d\omega. \tag{58}$$

Here  $\mathcal{C}_-$  is a contour running from  $-\infty$  along the lower edge of the left cut, turning around  $\omega = -\omega_{Ai}$ , and then running back to  $-\infty$  along the upper edge of the left cut (see Fig. 3). The contour  $\mathcal{C}_+$  runs from  $\infty$  along the upper edge of the right cut, turns around at  $\omega = \omega_{Ai}$ , and then runs back to  $\infty$  along the lower edge of the right cut.

The integral over the contour  $\mathcal{C}_-$  can be written as

$$\int_{\mathcal{C}_-} \frac{W_0(\omega)}{D(\omega; R)} e^{-i\omega t} d\omega = \int_{-\infty}^{-\omega_{Ai}} \left( \frac{W_0^-(\omega)}{D^-(\omega; R)} - \frac{W_0^+(\omega)}{D^+(\omega; R)} \right) e^{-i\omega t} d\omega, \tag{59}$$

where the superscripts “-” and “+” indicate the values of a function on the lower and upper edges, respectively, of the left cut. Using integration by parts, it is easy to show that the ratio of the integral on the right-hand side of equation (59) to the expression in the curly brackets on the right-hand side of equation (58) is of the order of  $(t\omega_k)^{-1}$  when  $t \gg \omega_k^{-1}$ . Similarly, we can obtain the same estimate for the integral over the contour  $\mathcal{C}_+$ . These two estimates enable us to neglect the second term on the right-hand side of equation (58).

Taking into account that  $\omega_d \approx \omega_k$  and  $D(\omega; R) \approx D_0(\omega)$ , we obtain

$$\text{res}_{\omega=\omega_d} \left( \frac{W_0(\omega)}{D(\omega; R)} e^{-i\omega t} \right) = -S e^{-i\omega_d t}, \quad (60a)$$

$$S = \frac{\rho^2 \omega_A^4 (\rho_i - \rho_e)^2 W_0(\omega_k)}{2\omega_k (\rho_i + \rho_e)^3}. \quad (60b)$$

We do not give the expression for  $W_0(\omega_k)$  because we do not use it in what follows. For the residue with respect to  $\omega = -\omega_d^*$  we obtain  $S^* e^{i\omega_d^* t}$ . As a result, we reduce equation (58) to

$$A(t) = i e^{-\gamma t} (S e^{-i\omega_d t} - S^* e^{i\omega_d^* t}) = 2|S| e^{-\gamma t} \sin(\omega_k t + \phi), \quad (61)$$

where we have written  $S$  as  $S = |S| e^{-i\phi}$ . We see that for  $t \gg \omega_k^{-1}$  the perturbation of the total pressure in the annulus oscillates harmonically with the frequency  $\omega_k$  and decays with the decrement  $\gamma$ , timescale  $\gamma^{-1}$ .

### 5.2. The Asymptotic State of the Boundary Oscillation

Let us study the asymptotic state of oscillations of the annulus boundaries. The velocities of the external and internal boundary are determined by equations (22) and (31), respectively. Using equations (21), (30), and (38)–(42), it is straightforward to show that  $\mathcal{L}[u_e]$  is regular at  $\omega = \pm\omega_{Ae}$  and  $\mathcal{L}[u_i]$  is regular at  $\omega = \pm\omega_{Ai}$ . This implies that the asymptotic behavior of  $u_e$  and  $u_i$  is determined by the contributions from the poles of  $\mathcal{L}[A]$  at  $\omega = \omega_d$  and  $\omega = -\omega_d^*$ . Using the same technique as in deriving equation (61), we obtain that, in the long-wavelength approximation ( $a \ll L$ ), this asymptotic behavior is given by

$$a u_e(t) = b u_i(t) = \Phi e^{-\gamma t} \cos(\omega_k t + \phi), \quad (62a)$$

$$\Phi = \frac{\rho \omega_A^2 (\rho_i - \rho_e) |W_0(\omega_k)|}{(\rho_i + \rho_e)^2}. \quad (62b)$$

Since  $b = a - \ell$ , we see that  $u_i = u_e + \mathcal{O}(\ell/a)$ , and the boundaries of the annulus oscillate with approximately the same velocity.

The quantities  $u_e$  and  $u_i$  are the complex amplitudes of the radial component of the velocity at  $r = a$  and  $r = b$ , respectively. The real radial velocity is given by  $\Re(u(r)e^{i\varphi}) = u(r) \cos \varphi$ . If we introduce the Cartesian coordinates  $x$  and  $y$  in such a way that  $\varphi$  is counted from the positive  $x$ -direction, then the radial velocities  $u_e \cos \varphi$  and  $u_i \cos \varphi$  correspond to the oscillations of the external and internal boundaries in the  $x$ -direction with the velocities  $u_e$  and  $u_i$ , respectively. We see from equation (62a) that the internal and external boundaries harmonically oscillate with the frequency of the global mode  $\omega_k$  and with amplitudes  $a^{-1}\Phi$  and  $b^{-1}\Phi$ , respectively. The relative difference in these amplitudes is of the order of  $\ell/a$ . Boundary oscillations decay with the decrement  $\gamma$ . Using equation (42), we obtain the estimate  $u_e \sim u_i \sim u_0$ .

## 6. MOTION IN THE DISSIPATIVE LAYER

In this section we study the motion in the dissipative layer embracing the ideal resonant position  $r = r_A$ . Since the dominant motion in the dissipative layer resides in the  $\varphi$ -

component of the velocity (e.g., Goossens et al. 1995; Goossens & Ruderman 1995), we study only the behavior of  $v$ .

Let us derive the expression for  $v$  in the annulus. We use the same method as in deriving equation (32). Introducing the notation  $V_1 = v$  and  $(2/\pi)g = -(i/r\rho)\partial P/\partial t$ , we rewrite equation (3b) in a form that exactly coincides with equation (13) by Ruderman (1999) with  $n = 1$  and  $\eta = 0$ . This enables us to write down the solution to equation (3b):

$$v = \exp(-\Lambda t^3/R) \left[ v_0 \cos(\omega_A t) + v_1 \frac{\sin(\omega_A t)}{\omega_A} \right] - \frac{i}{a\rho} \int_0^t G(t-\tau) \frac{dA}{d\tau} d\tau, \quad (63)$$

where  $G(t)$  is given by equation (33). We have used the facts that  $r \approx a$  and  $P(t, r) \approx A(t)$  in the annulus when deriving equation (63).

Substituting equations (33) and (57) into equation (63), introducing the new integration variable  $s = (t - \tau)\delta_\omega$ , and changing the order of integration, we obtain

$$v = \exp(-\Lambda t^3/R) \left[ v_0 \cos(\omega_A t) + v_1 \frac{\sin(\omega_A t)}{\omega_A} \right] - \frac{1}{4\pi a \rho \omega_A \delta_\omega} \int_{-\infty+i\epsilon}^{\infty+i\epsilon} \frac{\omega W_0(\omega)}{D(\omega; R)} \left[ \tilde{F}((\omega + \omega_A)/\delta_\omega, t\delta_\omega) - \tilde{F}((\omega - \omega_A)/\delta_\omega, t\delta_\omega) \right] e^{-i\omega t} d\omega, \quad (64)$$

where the function  $F$  is defined in equation (34). Using the same procedure as in deriving equation (61), we obtain that for  $t \gg \omega_k^{-1}$  the asymptotic behavior of  $v$  is given by

$$v = \exp(-\Lambda t^3/R) \left\{ v_0 \cos(\omega_A t) + v_1 \frac{\sin(\omega_A t)}{\omega_A} \right\} - \frac{i\omega_k e^{-\gamma t}}{a\rho \omega_A \delta_\omega} \Re \left\{ S e^{-\omega_k t} \left[ \tilde{F}((\omega_d - \omega_A)/\delta_\omega, t\delta_\omega) - \tilde{F}((\omega_d + \omega_A)/\delta_\omega, t\delta_\omega) \right] \right\}. \quad (65)$$

It is straightforward to obtain the estimate  $\delta_\omega \sim \omega_k (aL/R\ell^2)^{1/3}$ . For typical coronal loops,  $L \sim 100a$ . In what follows we take  $\ell \sim 0.1a$ . Then  $\delta_\omega \sim 20\omega_k R^{-1/3} \sim 20\gamma(a/\ell)R^{-1/3}$ . For typical coronal conditions,  $R \gtrsim 10^{12}$ , and so  $20(a/\ell)R^{-1/3} \ll 1$ . Thus,  $\omega_k/\delta_\omega \gg 1$  and  $\gamma/\delta_\omega \gg 1$ . Using integration by parts, we obtain the estimate

$$\tilde{F}((\omega_d + \omega_A)/\delta_\omega, t\delta_\omega) \sim \delta_\omega/\omega_k. \quad (66)$$

Another important estimate for what follows is  $(\gamma/\omega_k)R^{1/3} \sim \ell R^{1/3}/a \gtrsim 10^3$ . It was shown by Ruderman, Tirry, & Goossens (1995; see also Tirry & Goossens 1996 and Ruderman et al. 2000) that in the case where  $\gamma/\omega_k \gtrsim R^{-1/3}$ , the thickness of the dissipative layer is equal not to  $\delta_A$  but to  $\ell\gamma/\omega_k \sim \ell^2/a$ . Hence, in what follows we consider  $|r - r_A| \lesssim \ell^2/a$ . Then we can use the approximate formula similar to equation (51),

$$\omega_d - \omega_A \approx \frac{\Delta(r - r_A)}{2\omega_k} - i\gamma, \quad (67)$$

to evaluate the first term in the square brackets in equation (65). Using this formula, we immediately obtain that this term is of the order of or larger than  $t\delta_\omega$ . This estimate and

equation (66) imply that the second term in the square brackets and the terms proportional to  $v_0$  and  $v_1$  on the right-hand side of equation (65) can be neglected in comparison with the first term in the square brackets for  $t \gg \omega_k^{-1}$ . As a result, we rewrite equation (65) in the following approximate form:

$$v = -\frac{ie^{-\gamma t}}{a\rho\delta_\omega} \Re \left\{ Se^{-i\omega_k t} \int_0^{t\delta_\omega} \exp\left(i\delta_A^{-1}(r-r_A)s \operatorname{sgn} \Delta + s\gamma/\delta_\omega - s^3/3\right) ds \right\}. \quad (68)$$

Let us estimate the ratio of the third and second terms in the exponent in equation (68). We have

$$\frac{s^3/3}{s\gamma/\delta_\omega} \leq \frac{t^2\delta_\omega^3}{3\gamma} \sim t^2 \frac{8 \times 10^3 \omega_k^3 R^{-1}}{3(\ell/a)\omega_k} \sim 3 \times 10^4 t^2 \omega_k^2 R^{-1}. \quad (69)$$

Now we consider times  $t$  such that  $\omega_k^{-1} \ll t \ll 10^{-2}\omega_k^{-1}R^{1/2}$ . Note that  $10^{-2}R^{1/2} \sim R^{1/3}$  for  $R \sim 10^{12}$ . Then, in accordance with equation (69), we can neglect the term  $s^3/3$  in the exponent in equation (68) in comparison with the term  $s\gamma/\delta_\omega$ , and the integral in equation (68) is easily calculated. As a result we arrive at

$$v \approx -\frac{i}{a\rho} \Re \left\{ \frac{Se^{-i\omega_k t}}{\gamma + i\Delta(r-r_A)/(2\omega_k)} \times [\exp(i(r-r_A)\Delta t/(2\omega_k)) - e^{-\gamma t}] \right\}. \quad (70)$$

Using equation (60b), we obtain the estimate  $v \sim u_0 a/\ell$ , valid for  $t \gtrsim \gamma^{-1}$  (note that  $\gamma^{-1} \ll 10^{-2}\omega_k^{-1}R^{1/2}$  for  $R \gg 10^6$ ). Hence, during the characteristic time  $\gamma^{-1}$  of the global-mode damping, the amplitude of the wave motion in the dissipative layer increases from a value of order  $u_0$  to a value of order  $u_0 a/\ell$ . This increase occurs because of the energy flux from the global motions into the dissipative layer. Then the amplitude remains of the same order of magnitude at least up to the time satisfying  $t \ll 10^{-2}\omega_k^{-1}R^{1/2}$ .

Note that, in accordance with equation (70), the characteristic scale of variation of  $v$  in the dissipative layer decreases as  $1/t$ . This decrease corresponds to phase mixing of Alfvén oscillations that occurs because  $\omega_A$  depends on  $r$  and the neighboring magnetic field lines oscillate with different frequencies (e.g., Heyvaerts & Priest 1983; Wright 1992a, 1992b; Mann, Wright, & Cally 1995).

The behavior of  $v$  given by equation (68) was studied by Ruderman & Wright (2000). It was shown that, in the case where  $\gamma \gg \omega_k R^{-1/3}$ ,  $|v|$  takes its maximum value at  $r = r_A$  when  $t = t_m \approx 3\gamma^{-1} \ln(\gamma/\delta_\omega)$ . Since  $\delta_\omega \sim 20\gamma(a/\ell)R^{-1/3}$ , we obtain  $t_m \approx 15\gamma^{-1}$  for  $a/\ell \sim 0.1$  and  $R = 10^{12}$ – $10^{14}$ . This maximum value is of the order of  $au_0/\ell$ . After reaching its maximum value,  $|v|$  exponentially decreases on the characteristic timescale  $\omega_k^{-1}R^{1/3}$ . Phase mixing continues until a time of order  $(\gamma/\delta_\omega^3) \sim 10^{-2}\omega_k^{-1}R^{1/2}$ . At this time the characteristic spatial scale is of order  $10^2\ell R^{-1/2}$ , while the amplitude of oscillations is already exponentially small.

The analysis of this section is based on the estimate  $R \gtrsim 10^{12}$  obtained with the use of Braginskii formulae for the viscosity coefficients. However, the coronal viscosity can be enhanced orders of magnitude by, for example, turbu-

lence. In that case it is quite possible that, instead of the  $\gamma^{-1} \ll \omega R^{1/3}$ , we would have  $\gamma^{-1} \gtrsim \omega R^{1/3}$ . Then the dissipative layer would be quasi-stationary and described by the same formulae as in the case of stationary resonant absorption (e.g., Mok & Einaudi 1985).

## 7. APPLICATION TO CORONAL LOOP OSCILLATIONS

Formula (56) gives the calculated decay rate of oscillations in the kink mode. Its use may be conveniently illustrated by taking the density profile in the annulus in the form

$$\rho(r) = \frac{\rho_i}{2} \left[ (1 + \chi) - (1 - \chi) \sin \frac{\pi(2r + \ell - 2a)}{2\ell} \right], \quad a - \ell < r < a, \quad (71)$$

where  $\chi = \rho_e/\rho_i$ . Using equation (47), we obtain  $r_A = a - \ell/2$  and  $\rho_A = \rho_i(1 + \chi)/2$ . Then it follows from equations (50) and (56) that

$$\gamma = \frac{\omega_k \ell (1 - \chi)}{4a(1 + \chi)}. \quad (72)$$

In terms of the period  $\tau = 2L/c_k$  of the fundamental kink mode with wavenumber  $k = \pi/L$  and kink speed  $c_k (= \omega_k/k)$ , we obtain an oscillation decay rate  $\tau_{\text{decay}} (= \gamma^{-1})$  of

$$\tau_{\text{decay}} = \frac{2a\rho_i + \rho_e}{\pi\ell\rho_i - \rho_e} \tau. \quad (73)$$

We consider this result in relation to the observational data reported by Nakariakov et al. (1999). These authors reported a coronal loop oscillation with frequency  $\omega_k \approx 0.024 \text{ s}^{-1}$  ( $\tau = 256 \text{ s}$ ) and decrement  $\gamma \approx 0.0011 \text{ s}^{-1}$  ( $\tau_{\text{decay}} = 870 \text{ s}$ ). Taking  $\rho_i = 10\rho_e$ , we obtain from equation (72) that  $\ell/a \approx 0.23$ .

It follows from equation (72) (and more generally from eq. [56]) that the condition  $\gamma \ll \omega_k$  is equivalent to  $\ell \ll a$ . It can be shown that, in the general case where the density varies through the whole tube cross section, the condition  $\gamma \ll \omega_k$  is equivalent to  $|\Delta| \gg \omega_k^2/a$ . This inequality means that the characteristic scale of the density variation near the resonant position is much smaller than the tube radius. When this condition is not satisfied, all solutions to the dispersion equation corresponding to the kink oscillations have imaginary parts of the same order as real parts. As a result all tube perturbations damp aperiodically or almost aperiodically, and an external perturbation does not cause pronounced tube oscillations.

Hollweg & Yang (1988) also discussed damping of the kink mode by resonant absorption, in the ideal case. Their analysis was for a plane, but they applied it to a cylinder by replacing the perpendicular wavenumber by  $1/a$ . Surprisingly, their procedure gives results identical to equations (56) and (73). They concluded that under coronal conditions “the waves are very effectively damped with an  $e$ -folding time of only two wave periods.”

## 8. DISCUSSION AND CONCLUSIONS

In this paper we have studied the plane-polarized kink oscillations of a straight cylindrical magnetic tube with the footpoints embedded in a dense immovable plasma. We have assumed that the equilibrium plasma density varies

only in a thin annulus at the tube boundary, the density falling smoothly from a value  $\rho_i$  to a value  $\rho_e$  ( $< \rho_i$ ). We have used the cold plasma approximation in viscous MHD and restricted the analysis to the fundamental mode.

We have determined the time evolution of the magnetic pressure in the annulus in terms of a Bromwich integral, thus obtaining the global mode of the tube oscillation. The global oscillation is weakly damped and, for large values of the viscous Reynolds number  $R$ , the decrement is independent of  $R$  and proportional to the ratio of the thickness  $\ell$  of the annulus and the radius  $a$  of the tube. We have shown that this global mode describes the asymptotic state of tube motions for times much larger than  $\omega_k^{-1}$ , the inverse of the eigenmode frequency  $\omega_k$ .

We have also studied the wave motion in the dissipative layer embracing the ideal resonant position, which is determined by the condition that the global-mode frequency matches the local Alfvén frequency at this position. The theoretical results obtained here may be compared with observations of coronal loop oscillations.

The main conclusions of our analysis are as follows:

1. The asymptotic state of motion of an arbitrarily perturbed thin magnetic tube is a weakly damped harmonic oscillation with the frequency of the global mode.

2. The tube oscillation is damped because of the conversion of the energy of the global mode into the energy of local Alfvén oscillations in the dissipative layer located at the ideal Alfvén resonant position.

3. The decrement  $\gamma$  of the tube oscillation is independent of the Reynolds number  $R$  when  $R \gg 1$ , and  $\gamma/\omega_k$  is of order of  $\ell/a$ ; hence, the condition  $\gamma \ll \omega_k$  is equivalent to  $\ell \ll a$ .

4. After the characteristic damping time  $\gamma^{-1}$  of the tube oscillation, the energy of the tube oscillation is converted into the energy of Alfvén oscillations in the dissipative layer; at this time the amplitude of oscillations in the dissipative layer is of the order of  $a/\ell$  times the maximum amplitude of the tube oscillation.

5. Under the assumption  $\gamma/\omega_k \gg R^{-1/3}$ , as in applications to the solar corona, the amplitude of oscillations in the dissipative layer continues to grow until a time of order  $t_m$ ; there-

after, it exponentially decreases on the timescale  $\omega_k^{-1}R^{1/3}$ . For typical coronal conditions,  $t_m \approx 15\gamma^{-1}$ . The maximum amplitude of Alfvénic oscillations is of order  $a/\ell$  times the maximum amplitude of the tube oscillation.

6. The Reynolds number  $R$  affects only the behavior of wave motions in the vicinity of the ideal resonant position, so that we cannot here draw any conclusions about the value of the viscosity in the corona on the basis of observations of damping of the coronal loop oscillations. In the case where  $\gamma/\omega_k \gg R^{-1/3}$ , motions in this region are characterized by strong spatial oscillations in the radial direction. However, if because of certain physical processes (e.g., turbulence) the viscosity becomes anomalously large, so that  $\gamma/\omega_k \lesssim R^{-1/3}$ , then motions in the vicinity of the ideal resonant position are characterized by a monotonic spatial behavior in the radial direction. If future observations are able to resolve spatial scales down to a few percent of a loop radius, then it may prove possible to make qualitative estimates of the value of  $R$  on the basis of this difference in the character of wave motions in the vicinity of the resonant position.

The conclusion that the condition  $\gamma \ll \omega_k$  is equivalent to  $\ell \ll a$  is of particular importance. It implies that, in the case where the density varies through the whole tube cross section with a characteristic scale  $a$ ,  $\gamma \sim \omega_k$ , and an external perturbation does not cause pronounced tube oscillations. This fact may explain why coronal loop oscillations are so rarely observed.

There are indications that loop structure in general is multithreaded on a scale below the loop radius, so that  $\ell \ll a$  (Aschwanden et al. 1999). It is thus of interest to consider such small-scale loop structures; we may expect that resonant absorption will then occur not in one but in  $n$  resonant layers, and the damping rate will accordingly be scaled by a factor of order  $n\ell/a$ . A detailed calculation of the damping rate for such a model, and its comparison with observations, is a natural extension of the present study.

The authors acknowledge support of INTAS grant 97-31931.

#### REFERENCES

- Abramowitz, M., & Stegun, A. 1964, Handbook of Mathematical Functions (Washington, DC: National Bureau of Standards)
- Aschwanden, M. J., De Pontieu, B., Schrijver, C. J., & Title, A. M. 2002, Sol. Phys., 206, 99
- Aschwanden, M. J., Fletcher, L., Schrijver, C. J., & Alexander, D. 1999, ApJ, 520, 880
- Beaufumé, P., Coppi, B., & Golub, L. 1992, ApJ, 393, 396
- Berghmans, D., & Clette, F. 1999, Sol. Phys., 186, 207
- Boris, J. P. 1968, Ph.D thesis, Princeton Univ.
- Braginskii, S. I. 1965, in Rev. Plasma Phys., 1, 205
- Cally, P. S. 1986, Sol. Phys., 103, 277
- Davila, J. M. 1987, ApJ, 317, 514
- DeForest, C. E., & Gurman, J. B. 1998, ApJ, 501, L217
- De Moortel, I., Ireland, J., & Walsh, R. W. 2000, A&A, 355, L23
- Edwin, P. M., & Roberts, B. 1983, Sol. Phys., 88, 179
- Erdélyi, R., & Goossens, M. 1995, A&A, 294, 575
- Goossens, M., Hollweg, J. V., & Sakurai, T. 1992, Sol. Phys., 138, 233
- Goossens, M., & Ruderman, M. S. 1995, Phys. Scr., T60, 171
- Goossens, M., Ruderman, M. S., & Hollweg, J. V. 1995, Sol. Phys., 157, 75
- Grossmann, W., & Smith, R. A. 1988, ApJ, 332, 476
- Halberstaad, G., & Goedbloed, J. P. 1995, A&A, 301, 559
- Heyvaerts, J., & Priest, E. R. 1983, A&A, 117, 220
- Hollweg, J. V. 1987, ApJ, 312, 880
- . 1990, J. Geophys. Res., 95, 2319
- Hollweg, J. V., & Yang, G. 1988, J. Geophys. Res., 93, 5423
- Ineson, J. A. 1978, ApJ, 226, 650
- Kappraff, J. M., & Tataronis, J. A. 1977, J. Plasma Phys., 18, 209
- Lee, M. A., & Roberts, B. 1986, ApJ, 301, 430
- Mann, I. R., Wright, A. N., & Cally, P. S. 1995, J. Geophys. Res., 100, 19441
- Mok, Y., & Einaudi, G. 1985, J. Plasma Phys., 33, 199
- Molowny-Hobas, R., Wiehr, E., Balthasar, H., Oliver, R., & Ballester, J. L. 1999, in JOSO Annual Report '98, ed. A. Antalová, H. Balthasar, & A. Kucěra (Tatranská Lomnica: Astronomical Institute), 126
- Nakariakov, V. M. 2000, in AIP Conf. Proc. 537, Waves in Dusty, Solar, and Space Plasmas, ed. F. Verheest, M. Goossens, M. A. Hellberg, & R. Bharuthram (Melville: AIP), 264
- . 2001, in INTAS Workshop on MHD Waves in Astrophysical Plasmas, ed. J. L. Ballester & B. Roberts (Palma de Mallorca: Univ. Illes Balears), 79
- Nakariakov, V. M., & Ofman, L. 2001, A&A, 372, L53
- Nakariakov, V. M., Ofman, L., Deluca, E. E., Roberts, B., & Davila, J. M. 1999, Nature, 285, 862
- Ofman, L., & Davila, J. M. 1995, J. Geophys. Res., 100, 23427
- . 1996, ApJ, 456, L123
- Ofman, L., Davila, J. M., & Steinolfson, R. S. 1994, ApJ, 421, 360
- . 1995, ApJ, 444, 471
- Ofman, L., Nakariakov, V. M., & DeForest, C. E. 1999, ApJ, 514, 441
- Ofman, L., Romoli, M., Poletto, G., Noci, G., & Kohl, J. L. 1997, ApJ, 491, L111
- O'Shea, E., Banerjee, D., Doyle, J. G., Fleck, B., & Murtagh, F. 2001, A&A, 368, 1095
- Poedts, S., Belliën, A. J. C., & Goedbloed, J. P. 1994, Sol. Phys., 151, 271

- Poedts, S., & Goedbloed, J. P. 1997, *A&A*, 321, 935  
Poedts, S., & Kerner, W. 1991, *Phys. Rev. Lett.*, 66, 2871  
———. 1992, *J. Plasma Phys.*, 47, 139  
Rae, I. C., & Roberts, B. 1982, *MNRAS*, 201, 1171  
Robbrecht, E., Verwichte, E., Berghmans, D., Hochedez, J. F., Poedts, S., & Nakariakov, V. M. 2001, *A&A*, 370, 591  
Roberts, B. 2000, *Sol. Phys.*, 193, 139  
Ruderman, M. S. 1999, *ApJ*, 521, 851  
Ruderman, M. S., Oliver, R., Erdélyi, R., Ballester, J. L., & Goossens, M. 2000, *A&A*, 354, 261  
Ruderman, M. S., Tirry, W., & Goossens, M. 1995, *J. Plasma Phys.*, 54, 129  
Ruderman, M. S., & Wright, A. N. 2000, *Phys. Plasmas*, 7, 3515  
Sakurai, T., Goossens, M., & Hollweg, J. V. 1991, *Sol. Phys.*, 133, 227  
Schrijver, C. J., Aschwanden, M. J., & Title, A. M. 2002, *Sol. Phys.*, 206, 69  
Schrijver, C. J., & Brown, D. S. 2000, *ApJ*, 537, L69  
Sedlacek, Z. 1971, *J. Plasma Phys.*, 5, 239  
Steinolfson, R. S., & Davila, J. M. 1993, *ApJ*, 415, 354  
Stenuit, H., Keppens, R., & Goossens, M. 1998, *A&A*, 331, 392  
Stenuit, H., Tirry, W. J., Keppens, R., & Goossens, M. 1999, *A&A*, 342, 863  
Terradas, J., Oliver, R., & Ballester, J. L. 2001, *A&A*, 378, 635  
Tirry, W. J., & Goossens, M. 1996, *ApJ*, 471, 501  
Wright, A. N. 1992a, *J. Geophys. Res.*, 97, 6429  
———. 1992b, *J. Geophys. Res.*, 97, 6439